Letter

Prediction of novel effects in rotational nuclei at high speed

Jian-You Guo [ID]

School of Physics and Optoelectronic Engineering, Anhui University, Hefei 230601, China

A R T I C L E   I N F O

A B S T R A C T

The study of high-speed rotating matter is a crucial research topic in physics due to the emergence of novel phenomena. In this letter, we combined cranking covariant density functional theory (CDFT) with a similarity renormalization group approach to decompose the Hamiltonian from the cranking CDFT into different Hermite components, including the non-relativistic term, the dynamical term, the spin-orbit coupling, and the Darwin term. Especially, we obtained the rotational term, the term relating to Zeeman-like effect, and the spin-rotation coupling due to consideration of rotation and spatial component of vector potential. By exploring these operators, we aim to identify novel phenomena that may occur in rotating nuclei. Signature splitting, Zeeman-like effect, and spin-rotation coupling are among the potential novelties that may arise in rotating nuclei. Additionally, we investigated the observability of these phenomena and their dependence on various factors such as nuclear deformation, rotational angular velocity, and magnetic field-like strength.

1. Introduction

The investigation of the structure and property of matter under extreme conditions is an important research subject for physicists. With the development of accelerator facilities, particle detector systems, and techniques of nuclear spectroscopy, physicists have discovered many novel phenomena with unexpected features in atomic nuclei. These novel phenomena include neutron (proton) halos [1,2], energy level inversion [3,4], change of magic numbers [5–7], exotic radioactivity [8,9], high spin states [10,11], and others.

The high-spin states provide an important opportunity to investigate the microscopic mechanism of deformed shell structure, single-particle motion, and collective excitation. Since the discovery of backbending phenomenon in high spin states [12], the rotation excitation has become an active frontier. The backbending [12,13], band termination [14,15], signature inversion [16], superdeformed rotation [10,11], magnetic and antimagnetic rotations [17,18], and chiral rotation [19] have attracted worldwide attention.

To investigate the rotational properties and structures of deformed nuclei, as well as to understand the novelties associated with rotational excitations, physicists have developed a variety of theoretical models. They include the cranked Nilsson-Strutinsky method [20], the cranked shell model [21], the projected shell model [22], the tilted-axis cranking model [18], and density functional theories [23,24]. However, these models have limitations due to the breaking of time-reversal symmetry by the Coriolis operator and unpaired nucleons, which results in

time-odd components that are difficult to treat within a non-relativistic framework.

The self-consistent cranking covariant density functional theory (CDFT) has successfully described the rotational excitations of atomic nuclei [25,26], including the magnetic rotation, antimagnetic rotation, chiral doublet bands [19,27], and multiple chiral doublets [28–31], and it can handle time-odd fields corresponding to nonzero spatial component of the vector potential, which is important for understanding these novel phenomena. Additionally, the CDFT with point-coupling interactions was developed [32] and applied successfully to magnetic and antimagnetic rotations [33].

Although the cranking CDFT provides an excellent description of rotational excitations, including magnetic rotation, antimagnetic rotation, and chiral double bands, there are potential novel effects hidden within the cranking Dirac Hamiltonian that have not yet been fully revealed. The non-relativistic expansion of the conventional Dirac Hamiltonian has yielded several Hermitian operators of immense physical relevance, including the spin-orbit coupling operator, dynamical operator, and non-relativistic approximation. The acquisition of these operators has been instrumental in comprehending the shell structure of atomic nuclei, the origin of pseudospin symmetry, and its breaking mechanism [34–39]. Furthermore, it has also contributed to our understanding of nuclear proton radioactivity [40]. In addition, this expansion serves as a crucial link between non-relativistic and relativistic frameworks [41,42], facilitating a comparison between relativistic and non-relativistic density functionals [43]. This comparison is neces-

sitated by the incomplete comprehension of the roles and significance of various terms in both relativistic and non-relativistic energy density functionals.

Particularly, this expansion can assist in comprehending and revealing the novel effects concealed within the Dirac Hamiltonian. In our previous work [34], we performed an expansion of the Dirac equation using the similarity renormalization group (SRG) method for spherical systems. In 2014, we extended this expansion to deformed systems [37]. Following our scheme, an analytic expansion to the $1/M^4$ order was obtained in Ref. [44] compared to the improvement achieved by a so-called reconstituted SRG method. Furthermore, in Ref. [45], by replacing $1/M$ with $1/(M+S)$, an improved convergence was achieved through the SRG expansion of the Dirac equation.

To date, there has been no non-relativistic expansion of the cranking Dirac Hamiltonian. In this study, we aim to perform a non-relativistic expansion of the cranking Dirac Hamiltonian using the SRG method. Our goal is to gain insights into the novel effects in rotating nuclei and predict new effects related to rotation. The theoretical formalism is presented in section 2. The numerical details and results are presented in section 3. A summary is given in section 4.

2. Decomposition of cranking Dirac Hamiltonian with similarity renormalization group

To investigate the potential emergence of novel phenomena in high-speed rotating nuclei or neutron stars, we have applied the SRG method to decompose the Dirac Hamiltonian from the cranking CDFT. Within the cranking CDFT, the Dirac equation describing rotating nuclei is represented as:

$$H\psi = \varepsilon\psi, \tag{1}$$

with the Dirac Hamiltonian

$$H = \vec{\alpha} \cdot \vec{\pi} + \beta(M+S) + V - \vec{\Omega} \cdot \vec{J}, \tag{2}$$

where $\vec{\pi} = \vec{p} - \vec{V}$ and $\vec{J} = \vec{r} \times \vec{\pi} + \vec{\Sigma}$ with $\vec{\Sigma} = \frac{\hbar}{4i}\vec{\alpha} \times \vec{\alpha}$. The scalar potential $S(\vec{r})$ and vector potential $V_\mu(\vec{r})$ from the CDFT are represented in the following form:

$$S(\vec{r}) = g_\sigma \sigma(\vec{r}),$$

$$V(\vec{r}) = g_\omega \omega_0(\vec{r}) + g_\rho \tau_3 \rho_{30}(\vec{r}) + e\frac{1-\tau_3}{2}A_0(\vec{r}),$$

$$\vec{V}(\vec{r}) = g_\omega \vec{\omega}(\vec{r}) + g_\rho \tau_3 \vec{\rho}_3(\vec{r}) + e\frac{1-\tau_3}{2}\vec{A}(\vec{r}). \tag{3}$$

To reveal the underlying physics hidden in the cranking Dirac Hamiltonian, we transform it into a Schrödinger-like form using SRG. The initial Hamiltonian H is transformed by the unitary operator $U(l)$ according to

$$H(l) = U(l)HU^\dagger(l), \quad H(0) = H \tag{4}$$

where l is a flow parameter. Differentiation of Eq. (4) gives the flow equation as

$$\frac{d}{dl}H(l) = [\eta(l), H(l)], \tag{5}$$

with the generator $\eta(l) = \frac{dU(l)}{dl}U^\dagger(l)$. The choice of $\eta(l)$ is to make $H(l)$ diagonal in the limit $l \to \infty$. For the present Hamiltonian, it is appropriate to choose $\eta(l)$ in the form

$$\eta(l) = [\beta M, H(l)]. \tag{6}$$

In order to solve Eq. (5), the Hamiltonian $H(l)$ is presented as a sum of even operator $\varepsilon(l)$ and odd operator $o(l)$:

$$H(l) = \varepsilon(l) + o(l), \tag{7}$$

where the even or oddness is defined by the commutation relations of the respective operators, i.e., $\varepsilon(l)\beta = \beta\varepsilon(l)$ and $o(l)\beta = -\beta o(l)$. The system can be solved perturbatively by the expansions of $\varepsilon(\lambda)$ and $o(\lambda)$ as follows

$$\frac{1}{M}\varepsilon(\lambda) = \sum_{i=0}^{\infty}\frac{1}{M^i}\varepsilon_i(\lambda),$$

$$\frac{1}{M}o(\lambda) = \sum_{j=1}^{\infty}\frac{1}{M^j}o_j(\lambda). \tag{8}$$

As $\varepsilon(0) = \beta(M+S) + V - \vec{\Omega} \cdot \vec{J}$ and $o(0) = \vec{\alpha} \cdot \vec{\pi}$, there are

$$\varepsilon_0(0) = \beta, \varepsilon_1(0) = \beta S + V - \vec{\Omega} \cdot \vec{J}, \varepsilon_i(0) = 0, i \geqslant 2; \tag{9}$$

$$o_1(0) = \vec{\alpha} \cdot \vec{\pi}, o_i(0) = 0, i \geqslant 2. \tag{10}$$

With the initial conditions, we have obtained the diagonal Hamiltonian:

$$\varepsilon(\infty) = M\varepsilon_0(\infty) + \varepsilon_1(\infty) + \frac{1}{M}\varepsilon_2(\infty) + \frac{1}{M^2}\varepsilon_3(\infty) + \cdots \tag{11}$$

The diagonal part describing the positive energy states H can be written as

$$H = H_{NR} + H_{Dy} + H_{SO} + H_{Dw} + H_R + H_Z + H_{SR}, \tag{12}$$

where

$$H_{NR} = \frac{1}{2M}\vec{\pi}^2 + S + V,$$

$$H_{Dy} = -\frac{S}{2M^2}\vec{\pi}^2 + \frac{i\hbar}{2M^2}\nabla S \cdot \vec{\pi},$$

$$H_{SO} = +\frac{\hbar}{8M^2}\vec{\sigma} \cdot \left[\vec{\pi} \times \left(\vec{E}_S + \vec{E}_V\right) - \left(\vec{E}_S + \vec{E}_V\right) \times \vec{\pi}\right],$$

$$H_{Dw} = \frac{\hbar^2}{8M^2}\nabla \cdot \left(\vec{E}_s - \vec{E}_V + \vec{E}_\Omega\right),$$

$$H_R = -\vec{\Omega} \cdot \vec{j},$$

$$H_Z = -\frac{\hbar}{2M^2}(M-S)\vec{\sigma} \cdot \vec{B},$$

$$H_{SR} = -\frac{\hbar}{8M^2}\vec{\sigma} \cdot \left(\vec{\pi} \times \vec{E}_\Omega - \vec{E}_\Omega \times \vec{\pi}\right). \tag{13}$$

Here $\vec{E}_S = \nabla S$, $\vec{E}_V = -\nabla V$, and $\vec{E}_\Omega = \left(\vec{\Omega} \times \vec{r}\right) \times \vec{B}$ with the assumption $\vec{B} = \nabla \times \vec{V}$. The angular momentum $\vec{j} = \left(\vec{r} \times \vec{\pi} + \vec{s}\right)$. H_{NR} corresponds to the non-relativistic approximation. H_{Dy} is the dynamical term. H_{SO} represents the spin-orbital coupling. H_{Dw} is the Darwin term. H_R is the rotational term. The Zeeman effect is related to the operator H_Z. H_{SR} is claimed as the spin-rotation coupling.

In comparison with the non-relativistic expansion of the conventional Dirac Hamiltonian, it is important to note that there are three additional terms from the non-relativistic expansion of the cranking Dirac Hamiltonian: H_R, H_Z, and H_{SR}. H_R is responsible for the signature splitting, which has been studied before. For instance, the signature splitting and inversion in ^{78}Br, ^{131}Ba, and ^{133}Ce were investigated using the cranked-shell-model approach [46,47], while that in ^{86}Y was examined using tilted axis cranking relativistic mean-field theory [48]. However, H_Z and H_{SR} have not been previously explored in research. The physical effects caused by these two terms are novel and deserve special attention.

3. Novel phenomena in rotating nuclei

Based on the diagonal cranking Dirac Hamiltonian presented in Eq. (12), we delve into novel phenomena in rotating nuclei. In previous works [34,37], we explored the physical implications of terms H_{NR}, H_{Dy}, H_{SO}, and H_{Dw}, and elucidated their impacts on spin and pseudospin symmetries [35,36,38,39].
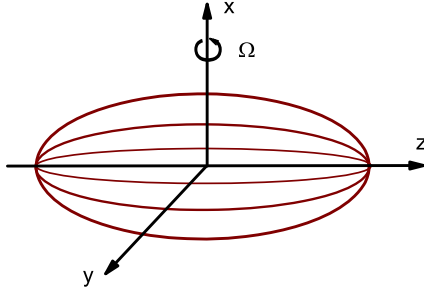
Fig. 1. An axially deformed nucleus rotating around x-axis. z is its symmetric axis. Ω is the rotational angular velocity.

As the rotation and spatial components of the vector field $\vec{V}(\vec{r})$ were not taken into account, H_R, H_Z, and H_{SR} did not appear in previous expansions. Although the physical effects of H_R have been studied before, non-relativistic expansions based on the cranking Dirac Hamiltonian have yet to be explored. Therefore, it is necessary to investigate the physical consequences of these additional terms and their contributions to single-particle spectra in atomic nuclei. For simplicity without loss of generality, we assume that the nucleus is symmetric around the z-axis, with rotation occurring around the x-axis. Additionally, a prolate or oblate deformation is considered in the z-axis direction, as illustrated in Fig. 1. The nucleus rotates around the x-axis with a rotational angular velocity Ω, i.e., $\vec{\Omega} = \Omega_x \vec{e}_x$. For the magnetic field-like $\vec{B}$, only the x-direction component $\vec{B} = B_x \vec{e}_x$ is considered. Under these assumptions, the Hamiltonian becomes the form.

$$H = \frac{\vec{\pi}^2}{2M} + \Sigma(r) - \Omega_x j_x$$
$$- \frac{S}{2M^2}\vec{\pi}^2 + \frac{i}{2M^2}\nabla S \cdot \vec{\pi} + \frac{1}{8M^2}\nabla^2 \Sigma$$
$$+ \frac{1}{4M^2}\vec{\sigma} \cdot \left(\nabla \Delta \times \vec{\pi}\right) - \frac{1}{2M^2}(M - S)\sigma_x B_x$$
$$+ \frac{B_x \Omega_x}{4M^2} + \frac{B_x \Omega_x}{4M^2}\vec{\sigma} \cdot \left(\vec{r}_{yz} \times \vec{\pi}\right). \tag{14}$$

In order to simplify computations and avoid affecting the conclusion, we have replaced $\vec{\pi}$ with $\vec{p}$. The energy spectra of the Hamiltonian in Eq. (14) are obtained through basis expansions. It is important to note that for axisymmetrically deformed nuclei, the third component of angular momentum is no longer a good quantum number due to rotation. Here, only axisymmetric quadruple deformation is considered, and parity remains a good quantum number. For illustration purposes, we have chosen ^{64}Ge as an example. To facilitate calculations, we have adopted scalar and vector potentials of the Woods-Saxon type, which are similar to the results obtained from RMF calculations. The corresponding potentials are represented as follows:

$$S(\vec{r}) = S_0(r) + S_2(r) P_2(\theta),$$
$$V(\vec{r}) = V_0(r) + V_2(r) P_2(\theta), \tag{15}$$

where $P_2(\theta) = \frac{1}{2}\left(3\cos^2\theta - 1\right)$. The radial parts in Eq. (15) take a Woods-Saxon form,

$$S_0(r) = S_{WS} f(r), \quad S_2(r) = -\beta_2 S_{WS} k(r),$$
$$V_0(r) = V_{WS} f(r), \quad V_2(r) = -\beta_2 V_{WS} k(r), \tag{16}$$

with $f(r) = \frac{1}{1+\exp\left(\frac{r-R}{a}\right)}$, and $k(r) = r\frac{df(r)}{dr}$. Here V_{WS} and S_{WS} are, respectively, the typical depths of the scalar and vector potentials in the relativistic mean field chosen as 350 and -405 MeV, the diffuseness of the potential a is fixed as 0.67 fm, and β_2 is the axial deformation parameter of the potential. The radius $R \equiv r_0 A^{1/3}$ with $r_0 = 1.27$ fm. With these parameters are determined, the energy spectra of Hamiltonian H can be calculated.
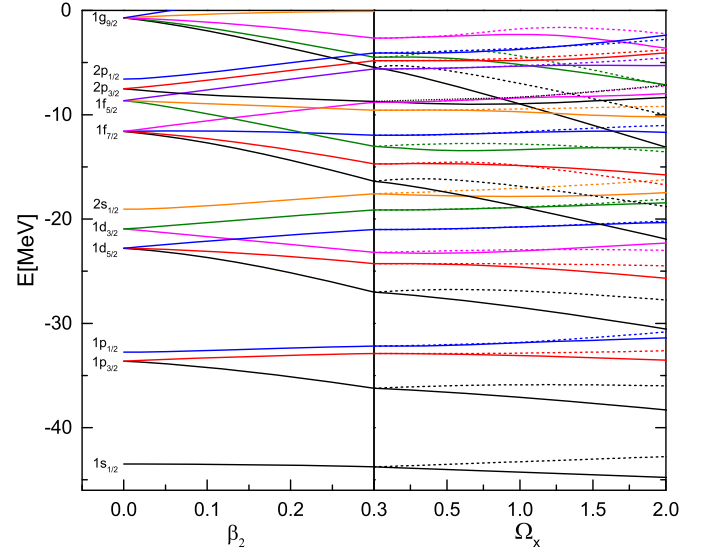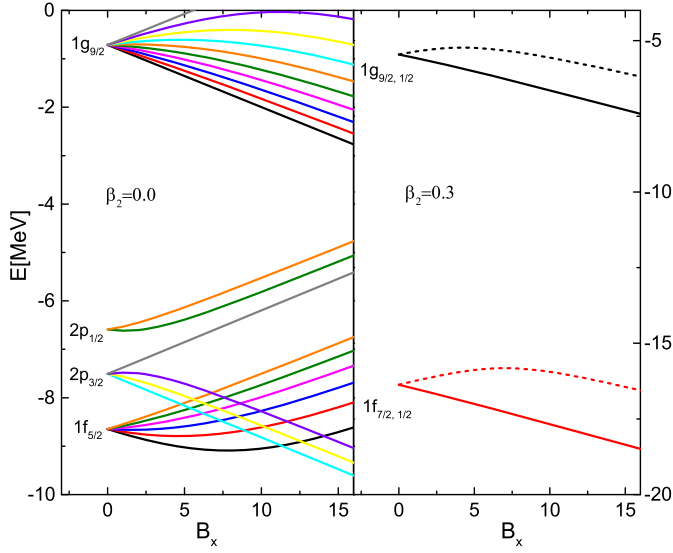

Fig. 2. The single-particle spectra and their evolutions to the quadruple deformation β_2 and the rotational angular velocity around x-axis Ω_x.

The single-particle spectra and their evolutions with the quadruple deformation β_2 and the rotational angular velocity around the x-axis Ω_x are presented in Fig. 2. The left panel shows the Nilsson levels with deformation β_2 ranging from 0 to 0.3. The right panel illustrates the variation of single-particle spectra with Ω_x for $\beta_2 = 0.3$. From the spherical to axial deformation, the levels experience splitting, as the well-known Nilsson levels are clearly visible. For axially deformed nuclei, there are signature splittings in doubly degenerate Nilsson levels. Compared to unaligned spin states, the signature splitting is larger for spin aligned states. In particular, for the spin aligned state with the least third component of total angular momentum, the signature splitting is the largest and most sensitive to Ω_x as shown in Fig. 2 for the single particle level $1g_{9/2,1/2}$. The single-particle energy drops faster with increasing Ω_x due to the stronger influence of the Coriolis force on the energy spectrum, which is consistent with the prediction of the cranking shell model. Signature splitting is an important phenomenon in rotating nuclei. The present calculations based on the diagonal Dirac Hamiltonian in Eq. (14) have reproduced the signature splitting.

In addition to the signature splitting caused by this cranking item H_R, the additional H_Z deserves special attention. It is the cause of the Zeeman effect in the atomic and molecular physics. To understand the role of H_Z in atomic nuclei, the single-particle spectra and their evolutions to the magnetic field-like B_x for the spherical nuclei and deformed nuclei with $\beta_2 = 0.3$ are presented in Fig. 3. In the left panel, the result for spherical nuclei is shown, while in the right panel, the results for deformed nuclei with $\beta_2 = 0.3$ are shown. When $B_x \neq 0$, every degenerate spherical level with the total angular momentum j is split into $2j + 1$ levels. As B_x increases, the level split increases as well. For deformed nuclei, the doubly degenerate Nilsson levels split when $B_x \neq 0$. The some splits are remarkable, while others are considerably small or even unobservable. However, for the spin aligned state with the least third component of total angular momentum, the level split is significant and sensitive to B_x, as seen in the right panel in Fig. 3 for $1f_{7/2,1/2}$ and $1g_{9/2,1/2}$. For the convenience of describing the problem, the splitting caused by the H_Z is claimed as Zeeman-like splitting. When B_x is large enough, the Zeeman-like splitting becomes considerable and may lead to an observable Zeeman-like effect. The observation of Zeeman-like effect can help us to understand the level structure and the strength of the magnetic field-like B_x. It is well worth experimentally probing the Zeeman-like effect in the nuclei.

Moreover, we have investigated the influence of the magnetic field-like B_x on signature splitting in rotating nuclei with $\beta_2 = 0.3$ and $\Omega_x = 2.0$ MeV. The left panel of Fig. 4 displays the level splittings for the
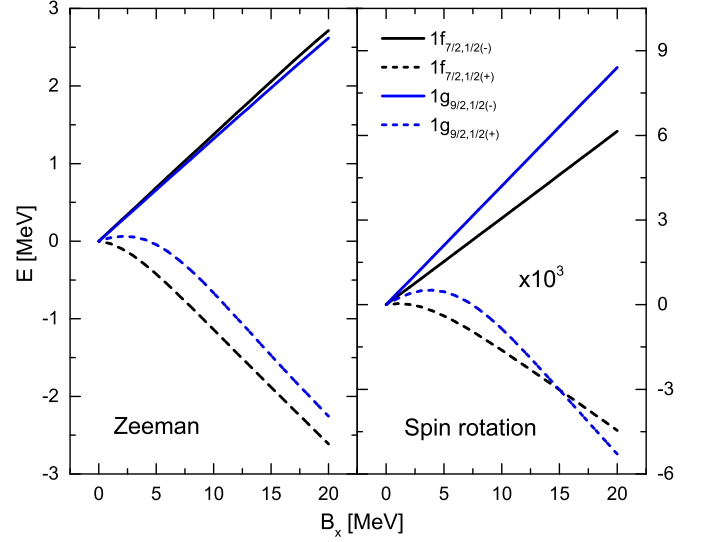
Fig. 3. The single-particle spectra and their evolutions to the magnetic field-like B_x for the spherical nuclei and deformed nuclei with $\beta_2 = 0.3$.
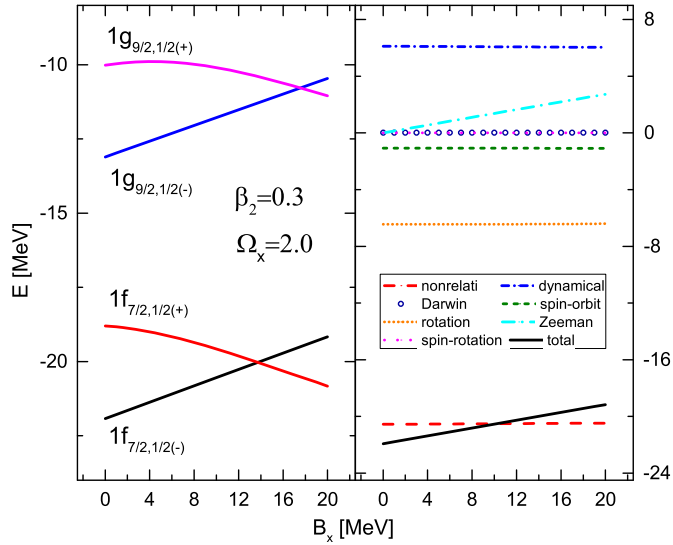
Fig. 4. The energies of single particle levels and their components evolve to the magnetic field-like B_x for the rotational nuclei with $\beta_2 = 0.3$ and $\Omega_x = 2.0$ MeV. The left panel shows the signature doublets $1f_{7/2,1/2}$ and $1g_{9/2,1/2}$. The right panel illustrates the contributions of every component to the single-particle level $1f_{7/2,1/2(-)}$.

signature doublets $1f_{7/2,1/2}$ and $1g_{9/2,1/2}$ and their evolutions to B_x. As B_x increases, the levels for the $1f_{7/2,1/2(-)}$ and $1g_{9/2,1/2(-)}$ go up, while those for the $1f_{7/2,1/2(+)}$ and $1g_{9/2,1/2(+)}$ go down. There are also the levels of the signature doublet crosses at a specific B_x. To clarify the evolution of level splittings to B_x, the contributions of every component to the single-particle level $1f_{7/2,1/2(-)}$ are displayed in the right panel of Fig. 4. The non-relativistic, dynamical, and rotational terms have significant contributions to the total energy. The spin-orbit coupling and the term relating to Zeeman-like effect contribute relatively little to the total energy. The Darwin term and the spin-rotation coupling contribute very little to the total energy. Except for the term relating to Zeeman-like effect, the other contributions to the total energy are independent of B_x. The energy increasing with B_x comes entirely from the contribution of the term relating to Zeeman-like effect, which is the cause of Zeeman-like effect in rotating nuclei.

Fig. 5. The energies contributed by the operator relating to Zeeman-like effect and the spin-rotation coupling, and their evolutions with the magnetic field-like B_x in the single particle levels $1f_{7/2,1/2(-)}$, $1f_{7/2,1/2(+)}$, $1g_{9/2,1/2(-)}$, and $1g_{9/2,1/2(+)}$. The other physical quantities are the same as Fig. 4.

To better understand the Zeeman-like effect in rotating nuclei, the left panel of Fig. 5 displays the signature splittings contributed by the term relating to Zeeman-like effect for the two signature doublets $1f_{7/2,1/2}$ and $1g_{9/2,1/2}$ with $\beta_2 = 0.3$ and $\Omega_x = 2.0$ MeV. With the increase of B_x, the energy increases for the $1f_{7/2,1/2(-)}$ and $1g_{9/2,1/2(-)}$, while the energy decreases for the $1f_{7/2,1/2(+)}$ and $1g_{9/2,1/2(+)}$. When $B_x = 20$ MeV, the increasing or reducing energy is about 3.0 MeV, which is quite observable. These indicate that the Zeeman-like effect plays a significant role in the signature splitting in rotating nuclei. For comparison, the spin-rotation coupling effect is displayed in the right panel in Fig. 5. The trend with B_x is similar, but the magnitudes are much smaller than 3 orders of magnitude.

4. Summary

In summary, we have combined the cranking CDFT with SRG to decompose the Dirac Hamiltonian into several Hermitian components, including the non-relativistic term, the dynamical term, and the spin-orbit coupling. Notably, we have considered the rotational and spatial components of the vector potential to obtain the rotational term, the term related to the Zeeman-like effect, and the spin-rotation coupling. Based on these operators, we have explored novel phenomena that may occur in rotating nuclei.

One of the most fascinating phenomena is signature splitting. Our findings indicate that signature splitting is more pronounced for spin-aligned states compared to unaligned spin states. Specifically, the spin-aligned state with the least third component and the largest total angular momentum experiences the largest signature splitting. The energy of this state decreases more rapidly with an increase in Ω_x, which can be attributed to the enhanced strength of the Coriolis force.

Furthermore, we have investigated the level splitting caused by the operator related to the Zeeman-like effect. For the spin-aligned state with the least third component, the level splitting is remarkable and sensitive to B_x. When B_x is sufficiently large, the Zeeman-like splitting becomes significant enough to produce an observable Zeeman-like effect for both spherical and deformed nuclei.

Moreover, we have examined the influence of the magnetic field-like B_x on signature splitting in rotating nuclei. We observed that as B_x increases, levels with the signature (-) go up while those with the signature (+) go down. This trend in level energies is entirely attributed to the contribution of the term related to the Zeeman-like effect.

The theoretical predictions on these novel phenomena have significant reference value for experimental detection of such phenomena in atomic nuclei.

Declaration of competing interest

Jian-You Guo declares that he has no known competing financial interests or personal relationships that could have appeared to influence the work reported in this paper.

Data availability

Data will be made available on request.

Acknowledgements

References

[1] I. Tanihata, H. Savajols, R. Kanungo, Prog. Part. Nucl. Phys. 68 (2013) 215.
[2] T. Nakamura, H. Sakurai, H. Watanabe, Prog. Part. Nucl. Phys. 97 (2017) 53.
[3] G.L. Wilson, et al., Phys. Lett. B 759 (2016) 417.
[4] B. Longfellow, D. Weisshaar, A. Gade, B.A. Brown, D. Bazin, K.W. Brown, B. Elman, J. Pereira, D. Rhodes, M. Spieker, Phys. Rev. Lett. 125 (2020) 232501.
[5] A. Ozawa, T. Kobayashi, T. Suzuki, K. Yoshida, I. Tanihata, Phys. Rev. Lett. 84 (2000) 5493.
[6] R.F. Garcia Ruiz, et al., Nat. Phys. 12 (2016) 594.
[7] E. Leistenschneider, et al., Phys. Rev. Lett. 126 (2021) 042501.
[8] E. Olsen, M. Pfützner, N. Birge, M. Brown, W. Nazarewicz, A. Perhac, Phys. Rev. Lett. 110 (2013) 222501;
Erratum, E. Olsen, M. Pfützner, N. Birge, M. Brown, W. Nazarewicz, A. Perhac, Phys. Rev. Lett. 111 (2013) 139903.
[9] Y.G. Ma, et al., Phys. Lett. B 743 (2015) 306.
[10] P.J. Twin, et al., Phys. Rev. Lett. 57 (1986) 811.
[11] B. Singh, R. Zywina, R.B. Firestone, Table of superdeformed nuclear bands and fission isomers: third edition (October 2002), Nucl. Data Sheets 97 (2002) 241.
[12] A. Johnson, H. Ryde, J. Sztarkier, Phys. Lett. B 34 (1971) 605.
[13] I.Y. Lee, M.M. Aleonard, M.A. Deleplanque, Y. El-Masri, J.O. Newton, R.S. Simon, R.M. Diamond, F.S. Stephens, Phys. Rev. Lett. 38 (1977) 1454.
[14] T. Bengtsson, I. Ragnarsson, Phys. Scr. T 5 (1983) 165.
[15] A. Afanasjev, D. Fossan, G. Lane, I. Ragnarsson, Phys. Rep. 322 (1999) 1.
[16] R. Bengtsson, H. Frisk, F.R. May, J.A. Pinston, Nucl. Phys. A 415 (1984) 189.
[17] S. Frauendorf, J. Meng, J. Reif, in: M.A. Deleplanque (Ed.), Proceedings of the Conference on Physics from Large γ-Ray Detector Arrays, University of California, Berkeley, 1994, p. 52, Report LBL35687, vol. II.
[18] S. Frauendorf, Rev. Mod. Phys. 73 (2001) 463.
[19] S. Frauendorf, J. Meng, Nucl. Phys. A 617 (1997) 131.
[20] G. Andersson, S.E. Larsson, G. Leander, P. Möller, S.G. Nilsson, I. Ragnarsson, S. Åberg, R. Bengtsson, J. Dudek, B. Nerlo-Pomorska, K. Pomorski, Z. Szymanski, Nucl. Phys. A 268 (1976) 205.
[21] R. Bengtsson, S. Frauendorf, Nucl. Phys. A 327 (1979) 139.
[22] H. Hara, Y. Sun, Int. J. Mod. Phys. E 04 (1995) 637.
[23] A.V. Afanasjev, J. König, P. Ring, L.M. Robledo, J.L. Egido, Phys. Rev. C 62 (2000) 054306.
[24] S. Sakai, K. Yoshida, M. Matsuo, Prog. Theor. Exp. Phys. 2020 (2020) 063D02.
[25] E. Ideguchi, et al., Phys. Rev. Lett. 87 (2001) 222501.
[26] D. Ray, A.V. Afanasjev, Phys. Rev. C 94 (2016) 014310.
[27] K. Starosta, et al., Phys. Rev. Lett. 86 (2001) 971.
[28] J. Meng, J. Peng, S.Q. Zhang, S.-G. Zhou, Phys. Rev. C 73 (2006) 037303.
[29] A.D. Ayangeakaa, et al., Phys. Rev. Lett. 110 (2013) 172504.
[30] I. Kuti, et al., Phys. Rev. Lett. 113 (2014) 032501.
[31] C. Liu, et al., Phys. Rev. Lett. 116 (2016) 112501.
[32] P.W. Zhao, Z.P. Li, J.M. Yao, J. Meng, Phys. Rev. C 82 (2010) 054319.
[33] J. Meng, P. Zhao, Phys. Scr. 91 (2016) 053008.
[34] J.Y. Guo, Phys. Rev. C 85 (2012) 021302(R).
[35] S.W. Chen, J.Y. Guo, Phys. Rev. C 85 (2012) 054312.
[36] D.P. Li, S.W. Chen, J.Y. Guo, Phys. Rev. C 87 (2013) 044311.
[37] J.Y. Guo, S.W. Chen, Z.M. Niu, D.P. Li, Q. Liu, Phys. Rev. Lett. 112 (2014) 062502.
[38] D.P. Li, S.W. Chen, Z.M. Niu, Q. Liu, J.Y. Guo, Phys. Rev. C 91 (2015) 024311.
[39] Bo Huang, Jian-You Guo, Shou-Wan Chen, Phys. Rev. C 105 (2022) 054313.
[40] Q. Zhao, J.M. Dong, J.L. Song, W.H. Long, Phys. Rev. C 90 (2014) 054326.
[41] H. Liang, S. Shen, P. Zhao, J. Meng, Phys. Rev. C 87 (2013) 014334.
[42] S. Shen, H. Liang, P. Zhao, S. Zhang, J. Meng, Phys. Rev. C 88 (2013) 024311.
[43] Z.X. Ren, P.W. Zhao, Phys. Rev. C 102 (2020) 021301(R).
[44] Yixin Guo, Haozhao Liang, Phys. Rev. C 99 (2019) 054324.
[45] Z.X. Ren, P.W. Zhao, Phys. Rev. C 100 (2019) 044322.
[46] E. Landulfo, D.F. Winchell, J.X. Saladin, F. Cristancho, D.E. Archer, J. Döring, G.D. Johns, M.A. Riley, S.L. Tabor, V.A. Wood, S. Salém-Vasconcelos, O. Dietzsch, Phys. Rev. C 54 (1996) 626.
[47] B. Ding, C.M. Petrache, S. Guo, E.A. Lawrie, I. Wakudyanaye, Z.H. Zhang, et al., Phys. Rev. C 104 (2021) 064304.
[48] J. Li, C.Y. He, Y. Zheng, C.B. Li, K.Y. Ma, J.B. Lu, Phys. Rev. C 88 (2013) 014317.